Article

Electrochemosensor for trace analysis of perfluorooctane sulfonate in water based on a molecularly imprinted poly o-phenylenediamine polymer

Najmeh Karimian, Angela Maria Stortini, Ligia Maria Moretto, Claudio Costantino, sara bogialli, and Paolo Ugo

ACS Sens., **Just Accepted Manuscript** • DOI: 10.1021/acssensors.8b00154 • Publication Date (Web): 18 Jun 2018

Electrochemosensor for trace analysis of perfluorooctane sulfonate in water based on a molecularly imprinted poly o-phenylenediamine polymer

Najmeh Karimian [1], Angela M. Stortini [1], Ligia M. Moretto [1], Claudio Costantino [1], Sara Bogialli [2], Paolo Ugo [1]*

[1] Department of Molecular Sciences and Nanosystems, University Ca' Foscari of Venice, via Torino 155, 30172 Venezia Mestre, Italy

[2] Department of Chemical Sciences, University of Padova, via F. Marzolo, 1, 35131 Padova, Italy

*Corresponding author: ugo@unive.it

ABSTRACT: This work is aimed at developing an electrochemical sensor for the sensitive and selective detection of trace levels of perfluorooctane sulfonate (PFOS) in water. Contamination of waters by perfluorinated alkyl substances (PFAS) is a problem of global concern due to their suspected toxicity and ability to bioaccumulate. PFOS is the perfluorinated compound of major concern, as it has the lowest suggested control concentrations. The sensor reported here is based on a gold electrode modified with a thin coating of a molecularly imprinted polymer (MIP), prepared by anodic electropolymerization of o-phenylenediamine (o-PD) in the presence of PFOS as the template. Activation of the sensor is achieved by template removal with suitable a solvent mixture. Voltammetry, a quartz crystal microbalance, scanning electron microscopy and elemental analysis were used to monitor the electropolymerization process, template removal and binding of the analyte. Ferrocenecarboxylic acid (FcCOOH) has been exploited as an electrochemical probe able to generate analytically useful voltammetric signals by competing for the binding sites with PFOS, as the latter is not electroactive. The sensor has a low detection limit (0.04 nM), a satisfactory selectivity, and is reproducible and repeatable, giving analytical results in good agreement with those obtained by HPLC-MS/MS analyses.

Keywords: perfluorooctane sulfonate, perfluoroalkyl substances, molecular imprinting, electrochemical sensor, environmental electroanalysis

The introduction of new consumer products and novel industrial processes means that many new chemicals are now found in the environment or in living organisms and are novel sources of environmental contamination [1-4]. The risk these chemicals pose to human health and to the environment is not yet fully understood, so they are classified as "emerging contaminants"; this class includes pharmaceutical and personal care products, endocrine disruptors, drugs of abuse and poly/perfluorinated substances (PFAS).

Thanks to their unique chemical properties, which include such as their hydrophobic character and remarkable chemical stability, PFAS have been widely produced and used as coatings for textiles, paper, food packaging and pots as well as additives in fire-fighting foams, lubricants, and other products [5]. These compounds are persistent in the environment and can be present at high concentrations in polluted areas for years, after their production or use was stopped.

Perfluorooctane sulfonate (PFOS) is one of the most widely used PFAS, and it is also suspected to be the most toxic [6-7]. For these reasons the use of PFOS has been restricted in Europe since 2006 [8]. Attention limits have been set for PFOS in waters, that differ slightly from country to country [9-11]. For instance, in 2016 the U.S. EPA's Office of Water indicated a lifetime health advisory limit of 70 ng/L (0.14-0.17 nM, depending on the prevailing species) for PFOS and pefluorooctanoic acid in drinking water [12], while, in Italy, a so-called *performance limit* for PFOS in ground and drinking waters was set at 30 ng/L (0.06 nM) [12-14]. Since these alarm limits are in the sub-nanomolar range, methods and devices for PFOS detection, must be extremely sensitive.

Usual analytical methods for detecting trace levels of PFAS (including PFOS) are based on highly sensitive but expensive HPLC-MS/MS methods [15-16]. However, when carrying out large-scale screening using decentralized methods of analysis, analytical devices need to be rapid, reliable and have a lower cost for first-level detection of the analyte.

Electrochemical sensors allow decentralized or automated analysis, since these devices combine high analytical selectivity and sensitivity with low cost and short analysis time [17]. To change voltammetric electrodes into environmental sensors, the device needs specific molecular recognition capabilities. This can be achieved by functionalizing the electrode surface with polymer films that can interact selectively with the analyte by complexation or ion-exchange [18-21]. An effective way to introduce specific chemical selectivity into a polymer layer is by the use of molecularly imprinted polymers (MIPs) [22-28]. Since the first studies on electrochemical MIP sensors in the 1990s [29-30], the

electroanalytical use of MIPs has progressively widened to a variety of analytes [31-35] including pollutants of environmental concern [36-38].

MIP-coated electrodes can be prepared by electropolymerization of suitable functional monomers in the presence of the analyte as a template molecule to form a cast-like shell. Suitable monomers should form complexes with the template through covalent or non-covalent interactions; the obtained structures are then stabilized by polymerization. Template removal generates three-dimensional cavities within the polymeric matrix which are complementary to the size, shape and functional groups of the target template/analyte [39]. Among the different methods for the synthesis of MIPs, the electropolymerization allows control of the MIP thickness by varying the electric charge used during deposition [40].

It should be noted that, in addition to their high affinity and selectivity for the target analyte [41], MIPs are characterized by high thermal and chemical stability, low cost and easy preparation

A further interesting feature of MIP-based electrochemical sensors is that they even allow detection of non-electroactive analytes, by exploiting the competition for the binding sites in the MIP between the analyte and a redox probe. The probe must have characteristics similar to the analyte as far as molecular size, ionic charge and binding interactions are concerned [42]; when operating under these experimental conditions, the probe signal will scale inversely with the analyte concentration.

Ortho-phenylenediamine (o-PD) has been widely applied for MIP preparation because it can be easily electro-polymerized onto various substrate materials producing stable ultrathin MIP films [35]. The presence of neutral or protonated $-NH_2$ groups facilitates interactions with oligodeoxyribonucleotides, enzymes or acidic analytes that can be used as molecular templates [43]. Therefore, o-PD is particularly suitable as a molecular mold, providing hydrophilic, hydrophobic, ionic and acid-base recognition sites [40]. MIP-based o-PD sensors have been developed for the detection of different analytes, including: troponin T [31], triclosan [44], sorbitol [45], oxytetracycline [46], glucose [47], dopamine [48], thrombin [49], gibberellin A3 [50], kojic acid [51].

As far as PFOS specific sensors are concerned, a fluorescent optical sensor [52] has been proposed, based on the functionalization of SiO_2 nanoparticles with a mixed layer of a fluorescein derivative and 3-aminopropyltriethoxisilane, whose amine functionalities interact with the sulfonic group of PFOS. An electrochemical biosensor was recently proposed, which exploited PFOS inhibition of the biocatalytic activity of an enzymatic biofuel cell [53], reaching a detection limit of 1.6 nM.

The development of an electrochemical sensor for PFOS is hindered by the lack of electroactivity of this analyte under normal experimental conditions [54]. Trying to overcome this problem, Tran et al.

proposed a photoelectrochemical PFOS sensor [55] based on a specialized platform of vertically aligned TiO_2 nanotubes, coated with molecularly imprinted polyacrylamide, synthesized by classical radical polymerization. The analyte is detected by exploiting the increase in photocurrent when PFOS interacts with the MIP coating. Unfortunately, all the PFOS sensors above have detection limits ≥ 1.6 nM, values that are higher than the subnanomolar levels required for monitoring PFOS in water samples.

In this work we present a different approach, where "classic" flat gold electrodes are functionalized with electropolymerized molecularly imprinted poly-o-PD, to improve both the detection capability and the general analytical applicability of the sensor. To overcome the lack of electrochemical activity of PFOS, ferrocenecarboxylic acid (FcCOOH) is used as a reversible redox probe, acting as a reporter molecule able to compete with PFOS for the molecularly imprinted recognition sites. It was observed that the FcCOOH voltammetric signal at the MIP coated electrode decreases progressively when the sensor is immersed in PFOS containing samples, scaling inversely with the PFOS concentration. Preparation of the sensor and the principles of PFOS determination are summarized in Scheme 1.

Here we present and discuss the preparation and characterization of the PFOS sensor and its analytical performance, with a focus on its application to monitoring trace concentrations of PFOS in water samples.

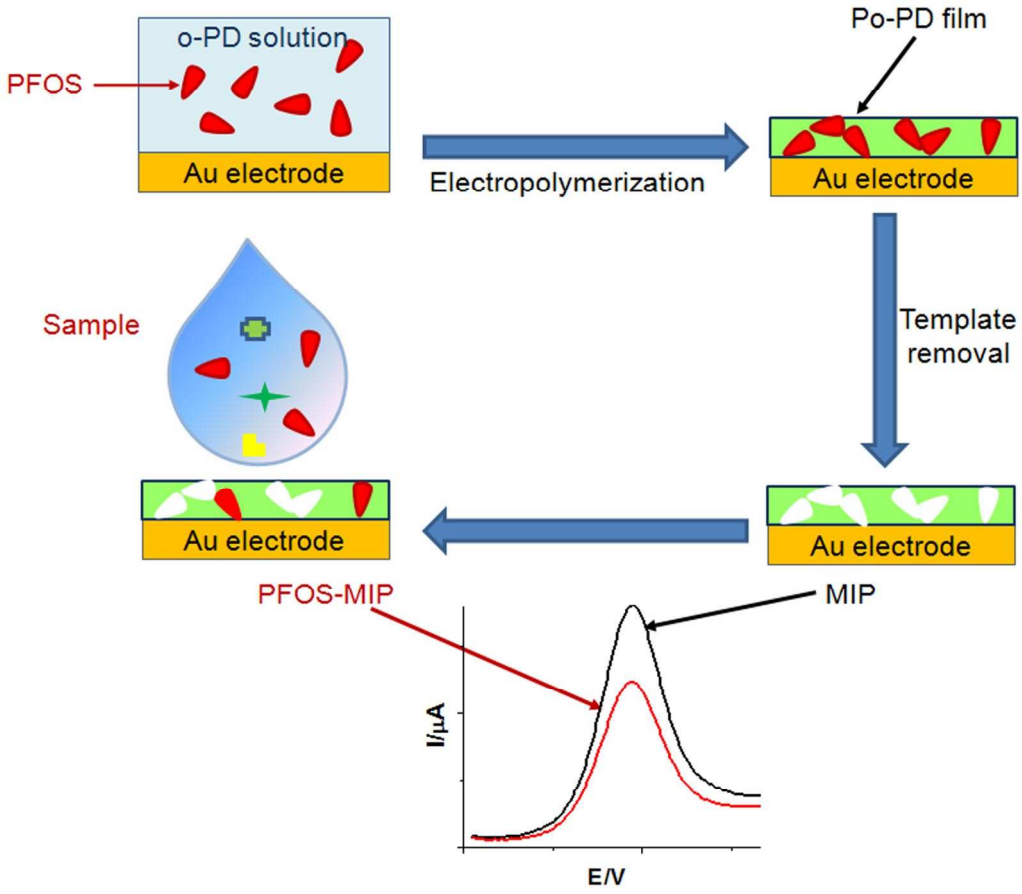

Scheme 1. Schematic representation of the molecular imprinting of the sensor and detection method.

Experimental section

Materials and apparatus. o-Phenylenediamine (o-PD, ≥98%), ferrocenecarboxylic acid (FcCOOH, ≥97%), perfluorooctane sulfonic acid potassium salt (PFOS, ≥98%), perfluorooctanoic acid (PFOA, ≥96%), perfluorohexane sulfonate (PFHxS, ≥98%), perfluorohexanoic acid (PFHxA, ≥97%), heptafluorobutyric acid (HFBA, 98%), perfluorobutanesulfonic acid (PFBS, 97%) were purchased from Sigma–Aldrich and 4-dodecyl benzene sulfonic acid (DBSA, ≥95%) from Fluka and were used as received.

A 0.5 M FcCOOH solution was prepared in 0.01 M ammonia buffer, at pH 8.4. All other reagents were of analytical grade and solutions were prepared using double distilled deionised water. All electrochemical measurements were carried out at room temperature with a CH660B potentiostat controlled via personal computer by its own software. A standard three-electrode configuration was used. The working electrode was a gold disk electrode (2.0 mm diameter), the counter electrode was a

platinum wire, the reference electrode was an Ag|AgCl|KCl (1 M), with respect to which all hereafter reported potential values are referenced. Scanning electron microscopy (SEM) and energy dispersive spectroscopy X-ray (EDX) analyses were performed using a TM3000 Hitachi tabletop scanning electron microscope coupled with a Swift ED3000 X-ray microanalysis system. Electrochemical quartz crystal microbalance (EQCM) measurements were performed using a QCA 917 SEIKO-EG&G in connection with a EG&G-PAR 273 potentiostat-galvanostat, controlled by the M270 software, using a 9 MHz AT-cut quartz crystal coated with gold (Au area 0.20 cm^2).

LC-MS analysis. The LC-MS was equipped with an Ultimate 3000 UHPLC chromatograph coupled with a hybrid quadrupole-Orbitrap™ Q-Exactive mass spectrometer (Thermo Fisher Scientific, Waltham, Massachusetts, USA). A Gemini NX-C18 3 µm, 110 Å, 100x2.0 mm (Phenomenex, Bologna, Italy) column thermostated at 15°C was used. Eluents were water (A) and acetonitrile (B) both containing 5 mM NH_4OH. At a flow rate of 0.2 mL/min, 100% of water was maintained for 2 min and then the chromatographic gradient was as follows: 2-15 min, 0-100% B; 15-20 min, 100% B; 20-21 min, 0% B; 21-28 min, 0% B. MS conditions were as follows: electrospray (ESI) ionization in negative mode, resolution 35000 in MS and 17500 in MS/MS, AGC target $3\cdot\times 10^6$ in MS and $2\cdot\times 10^5$ in MS/MS, max injection time of 200 and 100 ms, respectively, scan range 66.7-1000 a.m.u, isolation window 3.0 *m/z*, collision gas nitrogen, normalized collision energy (stepped) 20, 50 eV, acquisition in full scan with lock mass at *m/z* 112.9856 (formic acid dimer). Capillary voltage was 3.0 kV, capillary temperature 320 °C, sheath and auxiliary gas was nitrogen at 40 and 20 a.u., respectively. Calibration was performed with a standard solution purchased by Thermo Fisher Scientific (Pierce® ESI Negative Ion Calibration Solution). The software for analysis of MS data was Xcalibur 3.1TM (Thermo Fisher Scientific). The software for chromatographic control was the Dionex Chromeleon Mass Spectrometry 2.14 (Thermo Fisher Scientific).

Five µL of water samples were directly injected into HPLC-MS system. Tandem MS spectrum of the PFOS $[M-H]^-$ ion at *m/z* 498.9302 was collected. PFOS concentrations in water samples were quantified by using a five-point matrix-matched calibration curve, ranging from 0.5 to 20 nM, assayed in independent duplicates. The calibration curve was made by plotting the peak area related to the extracted ion chromatogram (accuracy 10 ppm) of the $[M-H]^-$ ion. MQ water was used as blank samples to verify the absence of systematic contamination. Linearity was evaluated through least squares regression and showed an R^2 of 0.9861, with an inter-day repeatability <15%, expressed as

RSD%. Under these experimental conditions, the LOD, evaluated as 3σ of the noise level of the blank samples (n=6), was estimated to be 0.5 nM for PFOS

Preparation of MIP and NIP sensors. The surface of the gold electrode was polished with 1.0, 0.3 and 0.05 μm wet alumina slurry and was then washed in an ultrasonic bath with doubly distilled water for 2 min. Then the potential was cycled between 0.2 and 1.5 V vs. Ag/AgCl in 0.5 M H_2SO_4 until a stable cyclic voltammogram was obtained. Electrosynthesis of the molecularly imprinted poly(o-phenylenediamine) (Po-PD) was performed by cyclic voltammetry (25 scans), by scanning the potential between 0 and 1.0 V vs. Ag/AgCl at 50 mV/s in a 0.1 M acetate buffer, pH 5.8/methanol (2:1, v/v) containing 10.0 mM o-PD in the presence of 1.0 mM PFOS. A control electrode modified with non-imprinted polymer (NIP) was obtained in the same way, but without PFOS addition as a template. The modified electrodes were dried under air flow and stored at room temperature.

Template removal. After polymerization, the modified electrode was rinsed with water and kept in methanol/water (1:1, v/v) solution for 20 min under mild stirring, followed by subsequent washing with methanol.

Electrochemical measurements. The interaction between PFOS and the MIP electrode was evaluated by immerging the electrode in a solution containing appropriate concentrations of PFOS, for 15 min with stirring. Electrochemical measurements to characterize the MIP electrode were carried out in a 0.5 mM FcCOOH solution (see above). Cyclic voltammograms (CVs) of the imprinted membranes were recorded within the potential range 0.0 - 0.5 V vs. Ag/AgCl, at a scan rate of 50 mVs^{-1}. For differential pulse voltammetry (DPV) the following optimized parameters were used: 0.0 V and 0.5 V vs. Ag/AgCl for the initial and final potential respectively; pulse width 25.0 ms; pulse amplitude 25.0 mV; increment potential 4.0 mV; scan rate 20 mVs^{-1}.

Results and discussion

Preparation of poly-o-PD coatings in the presence or absence of PFOS. A typical cyclic voltammogram recorded during the electropolymerization of o-PD in the presence of PFOS on a gold electrode is shown at Figure 1A. In the first scan an anodic peak was detected at approximately 0.36 V vs. Ag/AgCl, whose peak current decreased progressively in the following cycles. The multiscan voltammogram shown in Figure 1B for the oxidation of o-PD monomer in the absence of PFOS, is

characterized in the first cycle by one main oxidation peak at about 0.39 V, followed by a 2nd peak at 0.72 V, in agreement with data reported in the literature for the electropolymerization of pure o-PD [56]. Also in this case, peak currents decrease when increasing the number of CV cycles. For both cases, visual and optical microscopic observations (see Figure S-1) confirmed the deposition of a film on the gold surface.

For the MIP electrode, the electropolymerization was monitored by performing EQCM measurements. Data in Figure S-2 show a remarkable decrease of the resonance frequency was observed during synthesis, the decrease become progressively smaller as the number of voltammetric cycles increased. All these results agree with the anodic electrodeposition of a non-conducting (insulating) polymer film which progressively coats all the electrode surface. This is typical for electrodeposition of Po-PD both in the absence [56] and presence of eventual template host molecules [57]. The progressive blocking of the electrode/solution interface is expected during the formation of relatively thin coatings. This was confirmed for MIP, for which the profilometric measurements gave an average film thickness of 170 ± 10 nm (N=3) (see Figure S-3) after 25 voltammetric cycles of electropolymerization .

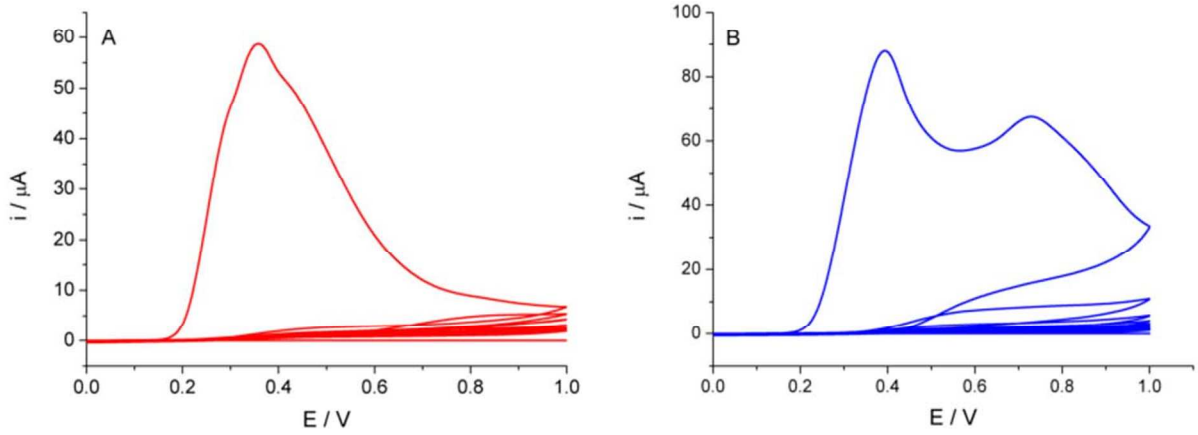

Figure 1. Cyclic voltammograms for the electropolymerization on a gold electrode in acetate buffer (pH 5.8). (A) containing 10 mM o-PD and 1 mM PFOS, (B) only 10 mM o-PD; scan rate 50 mVs^{-1}; number of scans 25.

Electrochemical characterization of the imprinted sensors. In previous studies on MIP sensors based on Po-PD [31, 57], ferricyanide was used as the electroactive redox probe for monitoring the uptake/release of the analyte into/from the imprinted recognition sites. When all the sites are saturated

with the analyte, the redox probe cannot reach the underlying Au surface of the electrode and no voltammetric signal is detected. On the other hand, when the recognition sites are accessible (no analyte) the redox probe generates its typical voltammetric signal.

Preliminary experiments, described in detail in the SI, indicated that ferricyanide is not the best probe for the repetitive monitoring of the uptake/release of PFOS from PFOS-imprinted-Po-PD (Figure S-4 and related text in SI). Satisfactory reproducibility was achieved when using ferrocenecarboxylic acid (FcCOOH) as the probe. Therefore, to characterize the MIP sensor, cyclic voltammograms were recorded in the presence of FcCOOH, which was chosen as the best electrochemical redox probe. The cyclic voltammogram (a) in Figure 2A shows the typical one-electron reversible oxidation of Fe(II) to Fe(III) of the FcCOOH molecule, recorded at a bare Au electrode [58]. The CV pattern (b) in the same Figure shows that the deposition of the MIP, prepared in the presence of PFOS, fully blocks electron transfer, the CV (c) shows that the FcCOOH was again detected after washing out the PFOS impregnated MIP with methanol/water (1:1, v/v). Voltammograms (d) to (i) in Figure 2B show that the FcCOOH signal recorded with the "washed" MIP electrode, decreased progressively when the MIP was incubated in solutions containing increasing concentration of PFOS.

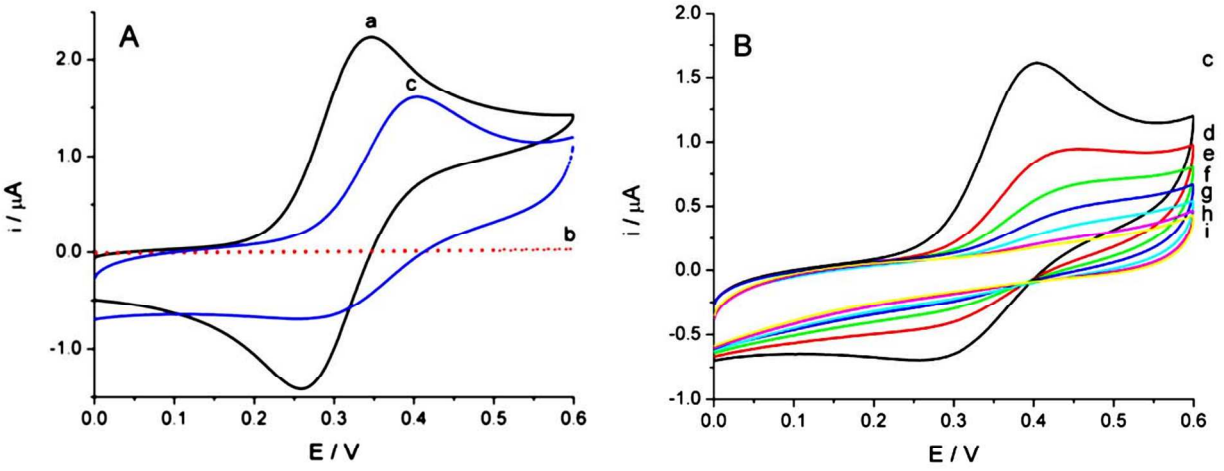

Figure 2. Cyclic voltammograms obtained with MIP electrode. (A): CVs of (a) bare Au electrode, (b) MIP-modified electrode, (c) MIP-modified electrode after removal of PFOS; (B): CVs of the MIP-modified electrode after 15 min incubation in 0.5 mM FcCOOH (pH 8.4) containing the following PFOS concentrations: (c) 0.0 nM, (d) 0.5 nM, (e) 1.0 nM, (f) 2.0 nM, (g) 5.0 nM, (h) 10.0 nM, (i) 50.0 nM. Scan rate: 50 mV s^{-1}.

EQCM measurements were performed by monitoring the change in frequency of a MIP (after template removal) and an NIP, prepared on a Au electrode on a quartz crystal, when dipped in PFOS solutions. The data reported in Figure S-5 show a notable decrease in the resonant frequency with dipping time for the MIP, while no frequency change was detected for the NIP.

These results indicate that washing the MIP with a methanol/water mixture is effective in removing the PFOS template, without damaging the polymer layer. Evidence that the MIP can efficiently upload PFOS after the washing, indicates that the PFOS recognition capability of the MIP remains unaltered. The upload-release of PFOS can be monitored repeatedly by following electrochemically the competition between the electro-inactive PFOS and the electroactive probe FcCOOH. Under the experimental conditions used for detection (buffer solution at pH 8.4) FcCOOH, whose pka is 6.7, is in the anionic carboxylated form [58], which means that both the analyte and the redox probe are good competitors since they both contain an anionic group bound to a relatively small hydrophobic backbone.

SEM-EDX characterization. By comparing the SEM images in Figure S-6 of a bare gold electrode (A) and an MIP (B), the successful deposition of a polymeric film on the gold surface is confirmed at the micrometer scale. Figure S-6C confirms that the polymeric film is still present after washing the MIP with methanol/water. Information on the elemental composition of the samples was obtained in the energy dispersive X-ray (EDX) spectra reported in Figure S-7. These data indicate the presence of S and F signals in the MIP before template removal (Figure S-7A), while, for the NIP, these signals were absent (Figure S-7B). After washing the MIP film with the extraction mixture (i.e. methanol/water), the disappearance of the S and F peaks was observed, confirming the removal of PFOS from the MIP (Figure S-7C).

Optimization of the sensor. To prepare an efficient MIP sensor with the best analytical performance, different influencing factors were investigated including: number of cycles for electropolymerization of o-PD; the monomer/template molar ratio (o-PD/PFOS); incubation time; and electrolyte pH. Details of the influence of these parameters are provided as Supporting Information (Figure S-8 and related text). To summarise, the optimized conditions are the following: electropolymerization: in the range 0.0 - 1.0 V vs. Ag|AgCl|KCl (1 M) for 25 cycles in acetate buffer (0.1 M, pH 5.8); monomer/template ratio: 10:1 (namely, 10.0 mM o-PD : 1.0 mM PFOS); PFOS

extraction time: 20 min in methanol/water (1:1, v/v), under mild stirring (followed by subsequent washing with methanol); PFOS rebinding: 15 min in ammonia buffer (0.01 M, pH 8.4) containing the analyte, with stirring.

Analytical performance and binding study. Quantitative analyses of PFOS using the MIP electrode prepared under optimized conditions, were performed using DPV. After template removal and background response measurements, MIP-modified electrodes were dipped in samples containing different concentrations of PFOS. As shown in Figure 3a, the peak current response decreased with increasing PFOS concentrations. Data plotted in Figure 3b indicate that the peak current decrease is proportional to the logarithm of the concentration of PFOS. However, in this plot two linear ranges can be identified, with different slopes: a higher slope in the concentration range 0.1 - 4.9 nM and lower between 9.5 nM and 1.5 μM.

The DPV data presented in the previous section were applied to study the binding properties of a MIP-modified electrode. We focused on the first part of the calibration range between 0.1 - 4.9 nM, where the highest affinity of the MIP for PFOS was observed. The change of current response of the FcCOOH probe (i_0-i) was calculated by subtracting the current recorded in the presence of PFOS (i) from the current recorded in the absence of PFOS (i_0) and was plotted against the PFOS concentration (Figure 3c). The binding isotherm of the MIP-modified electrode was fitted using a model that took into account the presence of two types of binding sites: specific recognition sites (in the polymer film) and non-specific sites on the surface of electrode, where non-specific adsorption could occur.

The model equation is the following:

$$i_0 - i = \frac{B_{MAX} c}{K_D + c} + N_S c \qquad (1)$$

where c is bulk concentration of the target, B_{MAX} is the maximum number of binding sites in the MIP, K_D is the equilibrium dissociation constant and N_S is the binding constant for nonspecific adsorption. The value K_D obtained from the fitting was 6.05×10^{-10} M (R^2 0.996), which confirmed PFOS had a high affinity for the recognition sites in the MIP.

Data in Figure 3c, confirm the trend observed in Figure 3b, that is, the sensitivity of the analysis decreases with increasing analyte concentration. This must be taken into account when performing quantitative analyses using standard addition methods, where the added PFOS concentration, must fall within a suitable linear portion of the calibration plot, and must be of the same order of magnitude as the analyte concentration in the investigated sample.

From the first data set in Figure 3c (i.e. PFOS concentration ≤ 1 nM) a detection limit (DL) of 0.04 nM was calculated using the equation DL= $3\sigma_b/m$, where σ_b is the blank standard deviation (namely, 10 nA, n=6) and m is the sensitivity (760 nA/nM).

The fabrication reproducibility of the imprinted electrodes was estimated as the relative standard deviation (RSD) of the PFOS concentration measured independently with three different MIP electrodes; at a PFOS concentration of 5.0 nM, it resulted equal to 7.7 %.

Concerning the measurement reproducibility with an individual sensor, a relative standard deviation (RSD) of 2.6 % was found from three successive measurements performed with the same MIP electrode, after regeneration with methanol/water before each measurement.

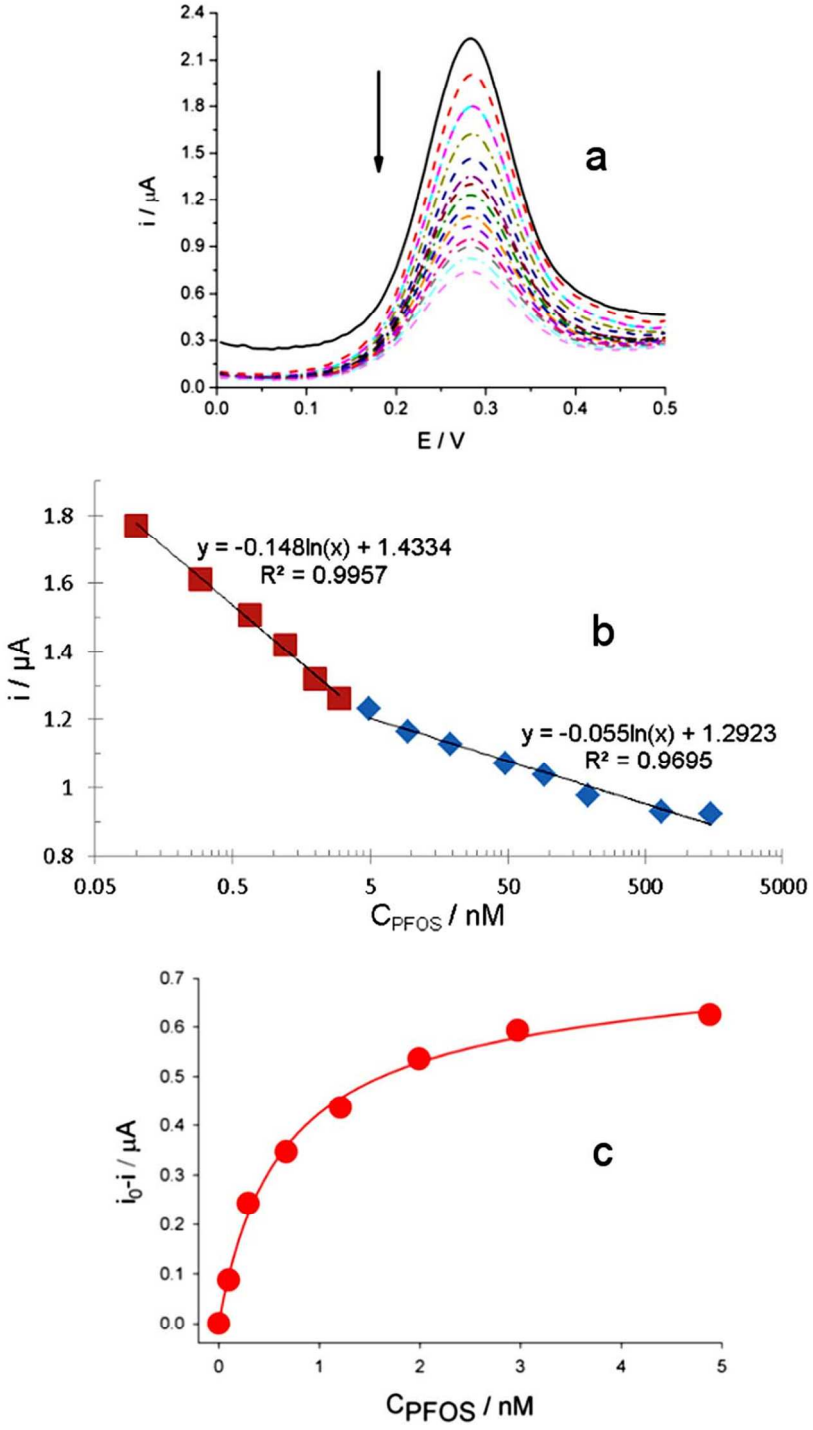

Figure 3. (a) DPVs at the MIP electrode after incubation in 0.5 mM FcCOOH (pH 8.4) containing different PFOS concentrations; full line: no PFOS added; dotted lines: samples containing increasing PFOS concentrations, from 0.1 nM to 1.5 µM (see abscissas axis in (b) for specific concentration values); (b) dependence of the peak current on the logarithm of the PFOS concentration; (c) binding isotherm of the MIP electrode at different concentrations of PFOS.

Selectivity of the imprinted sensor. The selectivity of the MIP-based sensor was evaluated by comparing the results obtained with the MIP sensor in 2nM PFOS solutions, in their absence and in the presence of possible interfering compounds, added in equimolar concentrations or in tenfold excess with respect to PFOS concentrations. We focused on anionic PFAS with 8, 6 or 4 carbon atoms, which can be present in PFOS contaminated waters, as well the widespread sulfonated surfactant 4-dodecyl benzene sulfonic acid. Slight variability between different MIP sensors was taken into account by normalizing changes in the (i_0-i) current with the relevant i_0 values (see above for definition of i_0 and i). The $[(i_0\text{-}i)/ i_0]_{PFOS + X}$ ratios were measured in 2nM PFOS in the presence of 2 or 20 nM of interferent X, where X = DBSA, PFOA, PFHxS, PFHxA, HBFA, or PFBS. These data were further normalized using the $[(i_0\text{-}i)/i_0]_{PFOS}$ ratio measured in 2 nM PFOS alone (with no added interference) and plotted to obtain the histogram shown in Figure 4.

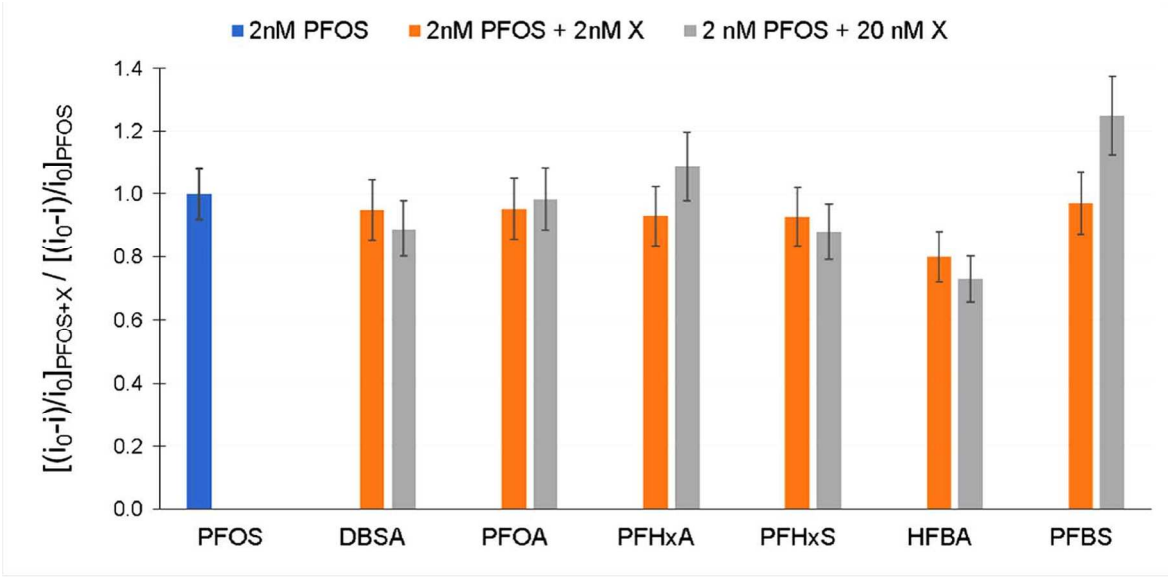

Figure 4. Histogram showing the ratio between normalized current recorded in 2 nM PFOS in the presence and absence of the interference X, where X = DBSA, PFOA, PFHxS, PFHxA, HFBA, PFBS.

These results indicate a small interferent effect for DBSA, PFOA, PFHxA, PFHxS where the normalized remained within 10 % of the reference value, even when the interfering substance was present in a tenfold excess of the PFOS concentration. A larger effect was observed for the smaller perflourinated anions HFBA and PFBS which when present in a tenfold excess, caused an

approximately 20 % change in the signal normalized to PFOS . This is not surprising since molecules smaller then PFOS (and with a similar molecular structure) can easily access the PFOS binding sites of the MIP, however the interference effects are quite limited. These results confirm that the MIP is characterized by a higher affinity for PFOS than for the examined competing interferences, even when the latter are present in an excess of one order of magnitude.

Water samples analysis. To verify the performance and applicability of the sensor, the MIP electrode was used to analyse water samples spiked with known amounts of PFOS as listed in the 2nd column of Table 1. These samples, before spiking, were determined to be PFOS-free by HPLC-MS/MS analyses. The concentration with the MIP sensor was determined using the standard addition method. DPVs were recorded under the same conditions as those described above in Figure 3. The results obtained with the MIP sensor are presented in the 3rd column in Table 1, where, for some samples, they are compared with data obtained by HPLC-MS/MS (4th column). The two data sets show a satisfactory agreement between the MIP and HPLC-MS results.

Since, presently no certified standard for trace PFOS in water is available, these results were taken as a proof of satisfactory trueness of the MIP based method. For all the spiked samples, recovery tests were performed by comparing the PFOS concentration measured with the MIP sensor with the amount added to distilled, tap and bottled mineral water. The recoveries were between 82 % and 110 %, indicating a satisfactory level of accuracy, which confirms the suitability of the sensor for practical application.

Table 1. PFOS concentrations measured with the MIP sensor and by HPLC-MS/MS

Sample	Spiked PFOS[1] (nM)	PFOS measured by MIP sensor (nM)	PFOS measured by HPLC-MS (nM)	Recovery (%) [3]
Distilled water	2.00	1.64 ± 0.20	n.m.[2]	82.0
	4.96	4.70 ± 0.17	n.m.[2]	94.7
Tap water	2.00	1.71 ± 0.10	n.m.[2]	85.5
Bottled mineral water	1.50	1.56 ± 0.09	1.52 ± 0.23	104.0
	1.80	1.77 ± 0.15	1.80 ± 0.24	98.3
	2.00	1.95 ± 0.18	n.m.[2]	97.5
	2.20	2.44 ± 0.2	2.22 ± 0.05	110.9
	3.20	3.18 ± 0.05	3.20 ± 0.01	99.4
	4.96	4.84 ± 0.28	n.m.[2]	97.6

1 Concentration of PFOS added to the sample, for which, initially, no PFOS was detected; these values correspond to the expected concentration.

2 n.m. = not measured

3 Calculated as $(C_{MIP}/C_{expected})$ x 100, where $C_{expected}$ and C_{MIP} are the concentration values reported in columns 2 and 3, respectively.

Conclusions In this study, an efficient electrochemical sensor for trace analysis of PFOS was obtained by electrodeposition of a molecularly imprinted polymer onto the surface of gold electrodes. Even if PFOS is not directly electroactive, we demonstrated that it can be detected electrochemically by competition for the molecular recognition sites of the MIP with a reporting electroactive probe,

namely ferrocenecarboxylic acid. It can be noted that this is the first time that such an approach has been used for sensing subnanomolar concentrations of a perfluorinated contaminant. The MIP-based sensor showed excellent analytical performance as far as sensitivity, detection limit and selectivity are concerned, furnishing analytical results comparable with those obtained by HPLC-MS/MS, even if the latter technique can allow multi analyte confirmatory detection. The results obtained indicate that the MIP sensor can be used for the rapid screening of PFOS in water samples, operating at concentration levels of real interest for environmental control, allowing the quick detection of a hazard situation related to PFOS contamination.

Associated Content

▪**Supporting Information.** The Supporting Information is available free of charge on the ACS Publications website. It includes Additional data and corresponding figures (PDF)

Acknowledgments

N.K. was the grateful recipient of a research grant supported partially by project PRIN 2010AXENJ8 (MIUR, Rome) and the University Ca' Foscari of Venice**.** C.C. was supported by FSE - Regione Veneto, grant code 2020/11/2016/2016.

References

1. Petriea, B.; Barden, R.; Kasprzyk-Hordern, B., A review on emerging contaminants in wastewaters and the environment: Current knowledge, understudied areas and recommendations for future monitoring. *Water Res.* **2015,** *72*, 3-27.

2. Geissen, V.; Mol, H.; Klumpp, E.; Umlauf, G.; Nadal, M.; Ploeg, M. v. d.; Zee, S. E. A. T. M. v. d.; Ritsema, C. J., Emerging pollutants in the environment: A challenge for water resource management. *ISWCR* **2015,** *3*, 57–65.

3. Kantiani, L.; Llorca, M.; Sanchís, J.; Farré, M.; Barceló, D., Emerging food contaminants: a review. *Anal. Bioanal. Chem.* **2010,** *398*, 2413–2427.

4. Farré, M.; Barceló, D.; Barceló, D., Analysis of emerging contaminants in food. *TrAC, Trends Anal. Chem.* **2013,** *43*, 240-253.

5. Vierke, L.; Staude, C.; Biegel-Engler, A.; Drost, W.; Schulte, C., Perfluorooctanoic acid (PFOA) — main concerns and regulatory developments in Europe from an environmental point of view. *Environ. Sci. Eur.* **2012,** *24*, 16-26.

6. Paiano, V.; Fattore, E.; Carra, A.; Generoso, C.; Fanelli, R.; Bagnati, R., Liquid Chromatography-Tandem Mass Spectrometry Analysis of Perfluorooctane Sulfonate and Perfluorooctanoic Acid in Fish Fillet Samples. *J. Anal. Methods Chem.* **2012,** *2012*, 1-5.

7. Lau, C.; Anitole, K.; Hodes, C.; Lai, D.; Pfahles-Hutchens, A.; Seed, J., Perfluoroalkyl acids: a review of monitoring and toxicological findings. *Toxicol. Sci.* **2007,** *99*, 366–394.

8. European Union, Restrictions on the marketing and use of certain dangerous substances and preparations (perfluorooctane sulfonates). Directive 2006/122/EC of the European Parliament and o Council. 12 December 2006

9. Pettersson, M.; Landell, M.; Ohlsson, Y.; Kleja, D. B.; Tiberg, C., Preliminary threshold values for highly fluorinated substances (PFAS) in soil and groundwater, Linkoping (in Swedish, English summary). Statens geotekniska institut, Linköping, Sweden: 2015.

10. Wilhelm, M.; Kraft, M.; Rauchfuss, K.; Holzer, J., Assessment and management of the first German case of a contamination with perfluorinated compounds (PFC) in the region Sauerland, North Rhine-Westphalia. *J. Toxicol. Environ. Health, Part A* **2008,** *71*, 725–733.

11. Guidance on the water supply (water quality) Regulations 2000 specific to PFOS (perfluorooctane sulphonate) and PFOA (perfluorooctanoic acid) concentrations in drinking water; DRINKING WATER INSPECTORATE, Whitehall, London 2009.

12. US EPA, Fact Sheet: PFOA and PFOS Drinking Water Health Advisories. https:// www.epa.gov/ground-water-and-drinking-water/drinking-water-health (in Italian) advisories PFOA and PFOS, 2016.

13. Italian Ministry of the Environmental, Legislative Decree, http://www.gazzettaufficiale.it/eli/id/2016/07/16/16A05182/sg (in Italian), 6 July 2016.

14. Veneto Regional Government, Decree 854, https://bur.regione.veneto.it/BurvServices/pubblica/DettaglioDgr.aspx?id=347691 (in Italian), 13 June 2017.

15. Larsen, B. S.; Kaiser, M. A.; Botelho, M.; Wooler, G. R.; Buxton, L. W., Comparison of pressurized solvent and reflux extraction methods for the determination of perfluorooctanoic acid in polytetrafluoroethylene polymers using LC–MS–MS. *Analyst* **2005,** *130*, 59–62.

16. Dasu, K.; Nakayama, S. F. M.; Yoshikane, M.; Mills, M. A.; Wright, J. M.; Ehrlich, S., An ultra-sesntivice method for the analysis of perfluorinated alkyl acids in drinking water using a column switching high-performance liquid chromatography tandem mass spectrometry. *J Chromatogr. A* **2017,** *1494*, 46-54.

17. Wang, J., Portable electrochemical systems. *TrAC, Trends Anal. Chem.* **2002,** *21*, 226-232.

18. Ugo, P.; Moretto, L. M., Ion exchange voltammetry at polymer-coated electrodes: priciples and analytical prospects. *Electroanalysis* **1995,** *7*, 1105-1113.

19. Brett, C. M. A.; Fungaro, D. A., Poly(ester sulphonic acid) coated mercury thin film electrodes: characterization and application in batch injection analysis stripping voltammetry of heavy metal ions. *Talanta* **2000,** *50*, 1223-1231.

20. Ugo, P.; Moretto, L. M.; Vezza, F., Ionomer-coated electrodes and nanoelectrode ensembles as electrochemical environmental sensors: recent advances and prospects. *Chem Phys Chem* **2002,** *3*, 917-925.

21. Kutner, W.; Wang, J.; L'her, M.; Buck, R. P., Analytical apects of chemically modified electrodes: Classification, critical evaluation and recommendations (IUPAC recommendations1998). *Pure Appl. Chem.* **1998,** *70*, 1302-1318.

22. Suryanarayanan, V.; Wu, C. T.; Ho, K. C., Molecularly Imprinted Electrochemical Sensors. *Electroanalysis* **2010,** *22*, 1795–1811.

23. Sharma, P. S.; Dabrowski, M.; D'Souza, F.; Kutner, W., Surface development of molecularly imprinted polymer films to enhance sensing signals. *TrAC, Trends Anal. Chem.* **2013,** *51*, 146-157.

24. Chen, L.; Wang, X.; Lu, W.; Wua, X.; Li, J., Molecular imprinting: perspectives and applications. *Chem. Soc. Rev.* **2016,** *45*, 2137-2211.

25. Wang, X.; Yu, S.; Liu, W.; Fu, L.; Wang, Y.; Li, J.; Chen, L., Molecular Imprinting Based Hybrid Ratiometric Fluorescence Sensor for the Visual Determination of Bovine Hemoglobin. *ACS Sens.* **2018,** *3*, 378–385.

26. Kamon, Y.; Takeuchi, T., Molecularly Imprinted Nanocavities Capable of Ligand-Binding Domain and Size/Shape Recognition for Selective Discrimination of Vascular Endothelial Growth Factor Isoforms. *ACS Sens.* **2018,** *3*, 580–586.

27. Guerreiro, J. R. L.; Bochenkov, V. E.; Runager, K.; Aslan, H.; Dong, M.; Enghild, J. J.; Freitas, V. D.; Sales, M. G. F.; Sutherland, D. S., Molecular Imprinting of Complex Matrices at Localized Surface Plasmon Resonance Biosensors for Screening of Global Interactions of Polyphenols and Proteins. *ACS Sens.* **2016,** *1*, 258–264.

28. Eersels, K.; Lieberzeit, P.; Wagner, P., A Review on Synthetic Receptors for Bioparticle Detection Created by Surface-Imprinting Techniques—From Principles to Applications. *ACS Sens.* **2016,** *1*, 1171–1187.

29. Hedborg, E.; Winquist, F.; Lundström, I.; Andersson, L. I.; Mosbach, K., Some studies of molecularly-imprinted polymer membranes in combination with field-effect devices. *Sens. Actuators, A* **1993,** *37–38*, 796-799.

30. Kriz, D.; Mosbach, K., Competitive amperometric morphine sensor based on an agarose immobilised molecularly imprinted polymer. *Anal. Chim. Acta* **1995,** *300*, 71–75.

31. Karimian, N.; Vagin, M.; Zavar, M. H. A.; Chamsaz, M.; Turner, A. P. F.; Tiwari, A., An ultrasensitive molecularly-imprinted human cardiac troponin sensor. *Biosens. Bioelectron.* **2013,** *50*, 492–498.

32. Yarman, A.; Turner, A. P. F.; Scheller, F., In *Nanosensors for chemical and biological applications*, Honeychurch, K. C., Ed. Woodhead: 2014; pp 125–149.

33. Gui, R.; Jin, H.; Guo, H.; Wang, Z., Recent advances and future prospects in molecularly imprinted polymers-based electrochemical biosensors. *Biosens. Bioelectron.* **2018,** *100*, 56-70.

34. Karimian, N.; Turner, A. P. F.; Tiwari, A., Electrochemical evaluation of troponin T imprinted polymer receptor. *Biosens. Bioelectron.* **2014,** *59*, 160–165.

35. Malitesta, C.; Losito, I.; Zambonin, P. G., Molecularly Imprinted Electrosynthesized Polymers: New Materials for Biomimetic Sensors. *Anal. Chem.* **1999,** *71*, 1366–1370.

36. Yang, Q.; Wu, X.; Peng, H.; Fu, L.; Song, X.; Li, J.; Xiong, H.; Chen, L., Simultaneous phase-inversion and imprinting based sensor for highly sensitive and selective detection of bisphenol A. *Talanta* **2018,** *176*, 595-603.

37. Zhang, J.; Wang, C.; Niu, Y.; Li, S.; Luo, R., Electrochemical sensor based on molecularly imprinted composite membrane of poly(o-aminothiophenol) with gold nanoparticles for sensitive determination of herbicide simazine in environmental samples. *Sens. Act. B* **2017,** *249*, 747-755.

38. Tan, F.; Cong, L.; Li, X.; Zhao, Q.; Quan, X.; Chen, J., An electrochemical sensor based on molecularly imprinted polypyrrole/graphene quantum dots composite for detection of bisphenol A in water samples. *Sens. Act. B* **2016,** *233*, 599-606.

39. Haupt, K., Plastic antibodies. *Nat. Mater.* **2010,** *9*, 612–614.

40. Malitesta, C.; Palmisano, F.; Torsi, L.; Zambonin, P. G., Glucose Fast-Response Amperometric Sensor Based on Glucose Oxidase Immobilized in an Electropolymerized Poly(o-phenyienediamine) Film. *Anal. Chem.* **1990,** *62*, 2735–2740.

41. Foguel, M. V.; Pedro, N. T. B.; Wong, A.; Khan, S.; Zanoni, M. V. B., Synthesis and evaluation of a moleculraly imprinted polymer for selective adsorption and quantification of Acid Green 16 textile dye in water samples. *Talanta* **2017,** *170*, 244–251.

42. Yarman, A.; Jetzschmann, K. J.; Neumann, B.; Zhang, X.; Wollenberger, U.; Cordin, A.; Haupt, K.; Scheller, F. W., Enzymes as Tools in MIP-Sensors. *Chemosensors* **2017,** *5*, 11-26.

43. Losito, I.; Palmisano, F.; Zambonin, P. G., o-Phenylenediamine electropolymerization by cyclic voltammetry combined with electrospray ionization-ion trap mass spectrometry. *Anal. Chem.* **2003,** *75*, 4988–4995.

44. Liu, Y.; Song, Q. J.; Wang, L., Development and characterization of an amperometric sensor for triclosan detection based on electropolymerized molecularly imprinted polymer. *Microchem. J.* **2009,** *91*, 222–226.

45. Feng, L.; Liu, Y.; Tan, Y.; Hu, J., Biosensor for the determination of sorbitol based on molecularly imprinted electrosynthesized polymers. *Biosens. Bioelectron.* **2004,** *19*, 1513–1519.

46. Li, J.; Jiang, F.; Wei, X., Molecularly Imprinted Sensor Based on an Enzyme Amplifier for Ultratrace Oxytetracycline Determination. *Anal. Chem.* **2010,** *82*, 6074–6078.

47. Cheng, Z.; Wang, E.; Yang, X., Capacitive detection of glucose using molecularly imprinted polymers. *Biosens. Bioelectron.* **2001,** *16*, 179–185.

48. Song, W.; Chen, Y.; Xu, J.; Yang, X. R.; Tian, D. B., Dopamine sensor based on molecularly imprinted electrosynthesized polymers. *J. Solid State Electrochem.* **2010,** *14*, 1909–1914.

49. Yang, S.; Li, L.; Zhang, X.; Shang, P.; Ding, S.; Zha, W.; Xu, W., Electrochemical determination of thrombin with molecularly imprinted polymers and multiwalled carbon nanotubes. *Can. J. Chem.* **2017,** *95*, 799-805.

50. Li, J.; Li, S.; Wei, X.; Tao, H.; Pan, H., Molecularly Imprinted Electrochemical Luminescence Sensor Based On Signal Amplification for Selective Determination of Trace Gibberellin A3. *Anal. Chem.* **2012,** *84*, 9951−9955.

51. Wang, Y.; Tang, J.; Luo, X.; Hu, X.; Yang, C.; Xu, Q., Development of a sensitive and selective kojic acid sensor based on molecularly imprinted polymer modified electrode in the lab-on-valve system. *Talanta* **2011,** *85*, 2522-2527.

52. Feng, H.; Wang, N.; Tran.T, T. T.; Yuan, L.; Li, J.; Cai, Q., Surface molecular imprinting on dye–(NH_2)–SiO_2 NPs for specific recognition and direct fluorescent quantification of perfluorooctane sulfonate. *Sens. Actuators, B* **2014,** *195*, 266–273.

53. Zhang, T.; Zhao, H.; Lei, A.; Quan, X., Electrochemcial biosensor for detection of perfluoroocatne sulfonate based inhibition biocatalysis of enzymatic fuel cell. *Electrochemistry* **2014,** *82*, 94-99.

54. Ochoa-Herrera, V.; Sierra-Alvarez, R.; Somogyi, A.; Jacobsen, N. E.; Wysocki, V. H.; Field, J. A., Reductive defluorination of perfluorooctane sulfonate. *Environ. Sci. Technol.* **2008,** *42*, 3260–3264.

55. Tran.T, T. T.; Li, J.; Feng, H.; Cai, J.; Yuan, L.; Wang, N.; Cai, Q., Molecularly imprinted polymer modified TiO_2 nanotube arrays for photoelectrochemical determination of perfluorooctane sulfonate (PFOS). *Sens. Actuators, B* **2014,** *190*, 745–751.

56. Losito, I.; Giglio, E. D.; Cioffi, N.; Malitesta, C., Spectroscopic investigation on polymer films obtained by oxidation of o-phenylenediamine on platinum electrodes at different pHs. *J. Mater. Chem.* **2001,** *11*, 1812-1817.

57. Karimian, N.; Zavar, M. H. A.; Chamsaz, M.; Turner, A. P. F.; Tiwari, A., On/off-switchable electrochemical folic acid sensor based on molecularly imprinted polymer electrode. *Electrochem. Commun.* **2013,** *36*, 92–95.

58. Silvestrini, M.; Schiavuta, P.; Scopece, P.; Pecchielan, G.; Moretto, L. M.; Ugo, P., Modification of nanoelectrode ensembles by thiols and disulfides to prevent non specific adsorption of proteins. *Electrochim. Acta* **2011,** *56*, 7718-7724.

for TOC only